Morphogenesis of 3D vascular networks is regulated by tensile forces

Dekel Rosenfeld[a], Shira Landau[a], Yulia Shandalov[a], Noa Raindel[a], Alina Freiman[a,b], Erez Shor[a], Yaron Blinder[a], Herman H. Vandenburgh[c], David J. Mooney[d,e], and Shulamit Levenberg[a,1]

[a]Department of Biomedical Engineering, Technion-Israel Institute of Technology, Haifa, 32000, Israel; [b]Interdepartmental Program in Biotechnology, Technion-Israel Institute of Technology, Haifa, 32000, Israel; [c]Department of Pathology and Laboratory Medicine, Brown University, Providence, RI 02906; [d]School of Engineering and Applied Sciences, Harvard University, Cambridge, MA 02138; and [e]Wyss Institute for Biologically Inspired Engineering, Harvard University, Boston, MA 02115

Edited by Robert Langer, Massachusetts Institute of Technology, Cambridge, MA, and approved February 9, 2016 (received for review November 11, 2015)

Understanding the forces controlling vascular network properties and morphology can enhance in vitro tissue vascularization and graft integration prospects. This work assessed the effect of uniaxial cell-induced and externally applied tensile forces on the morphology of vascular networks formed within fibroblast and endothelial cell-embedded 3D polymeric constructs. Force intensity correlated with network quality, as verified by inhibition of force and of angiogenesis-related regulators. Tensile forces during vessel formation resulted in parallel vessel orientation under static stretching and diagonal orientation under cyclic stretching, supported by angiogenic factors secreted in response to each stretch protocol. Implantation of scaffolds bearing network orientations matching those of host abdominal muscle tissue improved graft integration and the mechanical properties of the implantation site, a critical factor in repair of defects in this area. This study demonstrates the regulatory role of forces in angiogenesis and their capacities in vessel structure manipulation, which can be exploited to improve scaffolds for tissue repair.

mechanical forces | endothelial cells | vascularization | engineered tissue

Techniques to generate vascularized tissues bear significant clinical value in regenerative medicine because they ensure sufficient oxygen and nutrient supply within the host tissue, cardinal to transplant integration and survival (1–7). Recent works have attempted to optimize blood vessel network properties, such as geometry, maturity, and stability, by supplementing cultures with biological factors (8), biomaterials (9), and geometrical constraints (10, 11). Although mechanical forces play a central role in all biological processes and have been demonstrated to influence cell differentiation (12), shape (13), migration (14) and organization (15), they have yet to be comprehensively investigated in relation to vascular network assembly. These forces can include both external forces, in the form of shear stress or tensile and compression forces (16), as well as cell-induced contractile forces (17). Both external tensile forces and cell-induced forces act on the cell cytoskeleton and are mostly transmitted to the cell through the actomyosin pathway, adhesion sites, and cell stress fibers (18). In addition, several studies have reported measurement of cell-induced forces on their substrates (19) but have hardly focused on identifying a correlation between the level of cell-induced force and tubular network organization.

Distinct differences in vascular network morphology exist between tissue types, where, for example, vessels are aligned in parallel to muscle fibers but take on a radial organization in the retinal lumen (20). We hypothesized that tensile forces applied by and on the cells during network assembly play a central role in determining vascular network morphology and properties. Moreover, we hypothesized that implantation of a vascular network organized to match that of the implantation site will improve tissue integration and long-term outcomes. This study monitored the impact of tensile forces on vascular network morphology and properties. Although previous studies primarily examined the effect of such forces on endothelial monolayers or individual cells (21, 22), the present experimental setup used 3D systems and focused on tube formation and vascular network assembly. More specifically, the effect of cyclic and static tensile forces on network morphogenesis in engineered tissue constructs and their effect on tissue integration postimplantation were examined.

Results

Static Tensile Forces Influence Vascular Network Organization and Angiogenesis. A coculture of fibroblasts and endothelial cells (ECs) was seeded within fibrin gel fabricated uniaxially between two polydimethylsiloxane (PDMS) μposts (Fig. S1*A*) (23). The visually observed effects were quantified by application of a custom-designed image analysis program, based on the Hough transform function in Matlab, to calculate the orientation of the vessel structures (Fig. S2). The static tensile forces, induced by cellular contractile forces and gel shrinkage, triggered formation of vessel-like structures parallel to the stretching direction, consistent with cell actin fiber orientation (Fig. S1 *B* and *C*). On day 8, the highest level of forces (200 μN) was measured in gels embedded with cocultures of ECs and fibroblasts, compared with acellular gels (75 μN) or those containing ECs only (55 μN) (Figs. S1*D* and S2). The low levels of forces measured in cultures containing ECs only were ascribed to cell-induced gel degradation whereas the slight increase from baseline in forces measured in the cell-free gel on the first three days postseeding was likely due to gel shrinkage. The low levels of forces applied by ECs resonate with other studies that showed that these cells fail to organize into vessels in the

Significance

Sorely lacking are techniques to engineer tissue grafts bearing a means to receive adequate blood supply during implantation and after integration with host tissue. Efforts to optimize graft tissue vascularization have manipulated multiple factors but have placed little focus on the role of mechanical forces in blood vessel network assembly. The present work assessed the impact of cell-induced and externally applied forces on the morphology of vessel networks within engineered tissue constructs. Network quality, directly correlated with force intensity and vessel orientation, was tunable by application of different patterns of force. Implantation of grafts bearing networks arranged to match those in the implant site is expected to improve graft integration prospects, as well as their long-term viability and strength.

Author contributions: D.R., S. Landau, Y.S., H.H.V., D.J.M., and S. Levenberg designed research; D.R., S. Landau, Y.S., N.R., and A.F. performed research; E.S., Y.B., and H.H.V. contributed new reagents/analytic tools; D.R., S. Landau, Y.S., N.R., D.J.M., and S. Levenberg analyzed data; and D.R., S. Landau, Y.S., H.H.V., D.J.M., and S. Levenberg wrote the paper.

The authors declare no conflict of interest.

This article is a PNAS Direct Submission.

[1]To whom correspondence should be addressed. Email: shulamit@bm.technion.ac.il.

This article contains supporting information online at www.pnas.org/lookup/suppl/doi:10.1073/pnas.1522273113/-/DCSupplemental.

absence of supporting cells (24). The involvement of cell contractility in the formation of the vascular network was studied by inhibiting myosin II, a cytoskeletal protein responsible for force transmission within cells. Vessel quality was determined by assessing CD31 levels on day 8 of culture, using a roundness parameter, which rose with object elongation (*SI Materials and Methods*). Upon addition of the inhibitor, reduced cell-generated forces were observed along with damaged networks, lacking elongated vessel-like structures and actin fibers (Fig. 1 *A*, *II* and *B*). Y27632-mediated inhibition of rho-associated protein kinase (ROCK), an integral mediator of tail retraction, cortical tension, and cell forces, imparted a similar effect (Fig. 1 *A*, *III* and *B*). Cultures treated with SU5416, an endothelial cell-specific inhibitor of the vascular endothelial growth factor (VEGF)-2 receptor (25), displayed reduced network quality whereas fibroblast actin fibers remained straight and aligned. Although the inhibitor had no direct effect on the capacity of the fibroblasts to induce forces, the absence of an intact network resulted in decreased generated force, compared with the control (Fig. 1 *A*, *IV* and *B*). Moreover, DAPT, the γ-secretase inhibitor shown to inhibit Notch signaling (26) and to increase the number of tip cells within the EC population, did not affect total measured force intensity but shortened the time to achieve maximum force by 3 d (day 5 versus day 8 in untreated cells) (Fig. 1 *A*, *V* and *B*). This effect can be attributed to increased angiogenic sprouting induced by the heightened tip cell counts (26). In all of the examined conditions, cell density and viability within the gel were not influenced by the addition of inhibitor (Fig. S3). Measurement of the cell-induced forces generated after cell exposure to external static tensile forces demonstrated a direct correlation between the level of cell-induced forces and network morphology, with a positive correlation between force intensity and vessel elongation (Fig. 1*C*). We therefore aimed to examine the isolated effect of cell-induced forces on vascular network assembly, without concomitant application of static tensile forces. To this end, blebbistatin and Y26732 were added to 3D polymeric free-floating Gelfoam constructs seeded with EC and fibroblasts. The myosin II inhibitor fully arrested network formation, and vessel quality was lower compared with those within the nontreated scaffold (Fig. 2 *A* and *B*). The effect proved reversible because vascular networks began to reform 2 d after removal of blebbistatin (day 9) (Fig. 2*C*). In contrast, cells retained their ability to form vascular networks in the presence of the ROCK inhibitor Y27632. Unlike its response to conditions of static tensile forces in the fixated fibrin gel, the network of free-floating gels was enriched in the presence of Y27632, compared with the control (Fig. 2 *A* and *B*).

Because previous studies have shown that cyclic tensile forces can affect orientation at the endothelial cellular level (27, 28), we now set out to also examine their effect on vessel network morphology and orientation. To this end, 3D Gelfoam scaffolds cocultured with ECs and fibroblasts for 4 d were exposed to uniaxial cyclic stretching (10% strain and 1-Hz frequency). Vessel-like structures took on a diagonal orientation, symmetrically organized 30–60° to the stretching direction, consistent with the orientation of the cell actin fibers (Fig. 3 *A* and *B*). Image analysis performed on day 8, using the Hough transform function, demonstrated more vessels aligned 30–60° to the stretching direction (mean 20 compared with 10 in other directions). In the control group, no favored direction was observed (Fig. 3*C*). Lumen-like structures were identified in paraffin sections cut perpendicular to the stretching direction, attesting to the formation of tube-like structures (Fig. S4). Static stretch, applied within a self-designed fixation device (Fig. S5), on similar 3D Gelfoam constructs yielded results similar to those observed with the fixated fibrin gel, with vessel orientation parallel to the stretching direction, consistent with the orientation of the cell actin fibers (Fig. 3 *A* and *B*).

In efforts to characterize factors underlying the differential effects of cyclic versus static tensile forces on vessel orientation, we measured angiogenesis-related cytokine levels after exposure to various mechanical force regimens (Table S1 and Fig. S6). Static stretching induced a significant increase in tissue inhibitor of metalloproteinases (TIMP2), platelet-derived growth factor

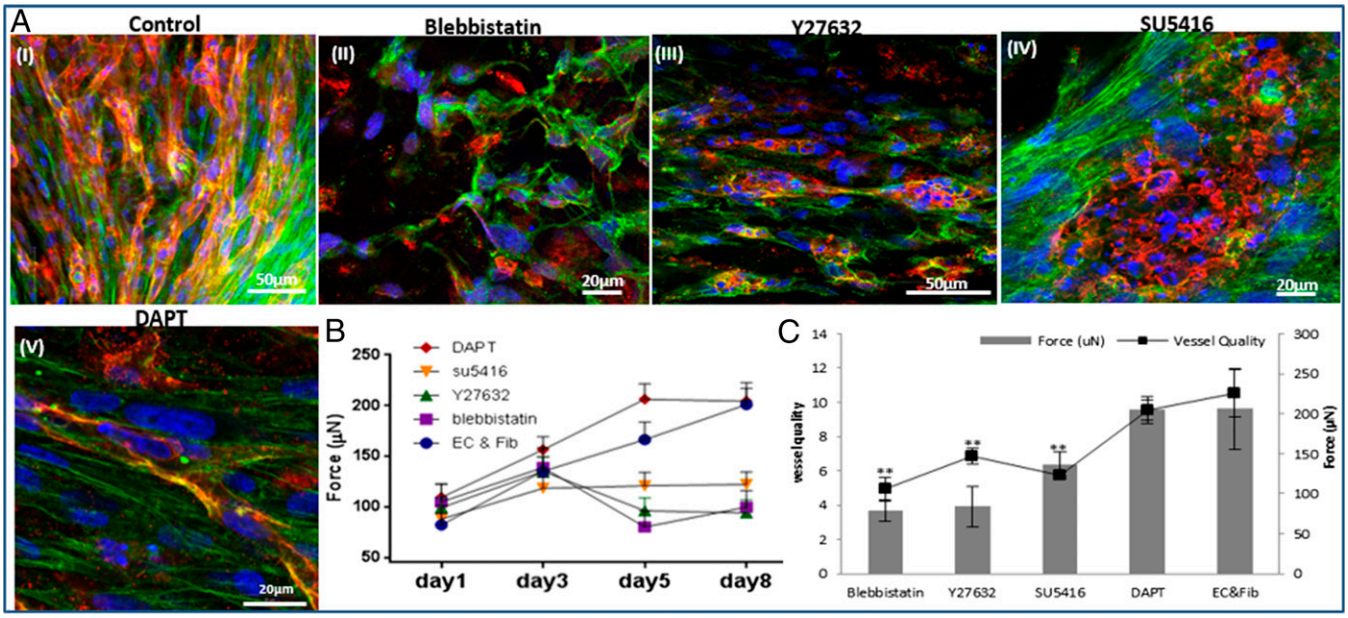

Fig. 1. The influence of cytoskeleton and intracellular signaling inhibitors on cell-induced contractile forces and vascular network formation. (*A*) Immunofluorescence imaging of a uniaxially fixated fibrin gel embedded with a coculture of endothelial cells and fibroblasts and grown for 8 d. Inhibitors were added to the culture medium on day 3 and replaced daily, along with the medium: (*I*) control gel, (*II*) gel treated with Blebbistatin, (*III*) gel treated with Y27632, (*IV*) gel treated with SU5416, and (*V*) gel treated with DAPT. Samples were stained to visualize the nuclei (DAPI, blue), endothelial cells (CD31, red), and actin fibers (Phalloidin-FITC, green). (*B*) Cell-induced contractile forces were measured as a function of μpost deflections of cell-embedded fibrin gels on days 1–8 postseeding. (*C*) A coplot of vessel quality and cell-induced contractile forces measured on day 8 postseeding.

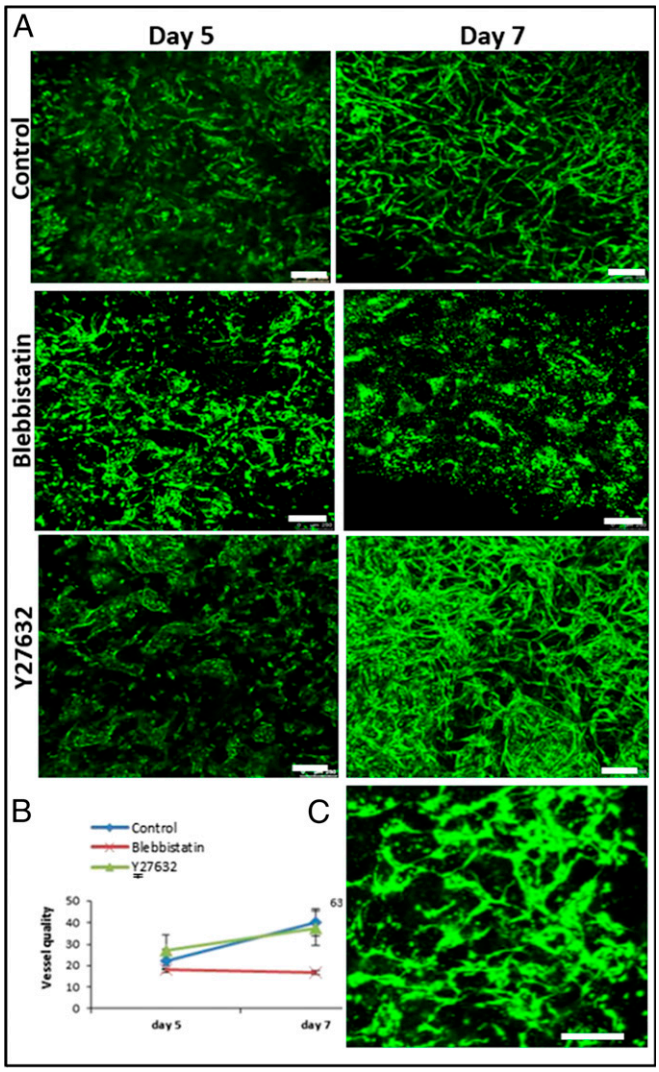

Fig. 2. Vascular organization within free-floating scaffolds upon inhibition of cell-generated forces. (*A*) HUVEC-GFP cells were embedded on a free-floating scaffold that was treated with an inhibitor (blebbistatin/Y27632) on day 3 of culture and later imaged on days 5 and 7. (Scale bars: 250 μm.) (*B*) Quantification of vessel quality determined by estimating the roundness parameter on days 5 and 7 postseeding. (*C*) Reformation of vascular networks on day 9, 2 d after removal of blebbistatin. (Scale bars: 250 μm.)

(PDGF-)-ββ, and angiopoietin-2 (ANG-2) expression levels, suggestive of accelerated network formation (21), whereas cyclic stretching triggered a significant increase in PDGF-ββ, VEGF, and TIMP1 expression levels, but to a decrease in TIMP2 (Fig.4).

Orientation of the Vascular Network Improves Integration upon Implantation. We aimed to evaluate the integration capacity of vessel-like structures designed to mimic the network orientation of the host tissue. To this end, scaffolds subjected to 8 d of static stretching were implanted into the mouse abdominal muscle in the linea-alba region, such that the stretching direction was parallel to the orientation of the mouse muscle fibers (Fig. S7*A*). Before implantation, no considerable differences were observed in the Young's modulus of the seeded constructs, when comparing stretching parallel to the aligned vessel direction and orthogonal to the aligned vessel direction. (Fig. S8). H&E staining of the scaffold area within the implantation site (retrieved post-implantation) demonstrated a connection formed between the host tissue and graft fibers (Fig. S7*B*). Two weeks postimplantation, functional blood vessels of both the host and the implanted vascular network were identified via rhodamine-dextran signals (red) (Fig. 5*A*). Histological analysis of samples retrieved at this time point (Fig. 5 *A*, *III*) demonstrated connections between mouse vessels and implanted human vessels. Moreover, vessel objects preserved their preimplantation orientation within the host (Fig. 5*B*), and functional vessel-like structures of static-stretched scaffolds were 2.5-fold longer compared with the control group of nonstretched nonoriented vessels (Fig. 5*C*).

To repair abdominal muscle defects, high stiffness must be achieved at the implantation site, to enable resistance of the high forces with which they are naturally challenged (2). To estimate the impact of oriented vessels on the mechanical properties of the host tissue, the engineered oriented vessel-like structures were implanted in parallel (vertical) vs. perpendicular (horizontal) to the muscle fibers and blood vessels of the host tissue (Fig. 6*A*). In addition, control grafts, with randomly organized vessels were implanted in a separate group of animals. The tissues with vertically implanted vessels demonstrated higher stiffness and higher ultimate tensile strength (UTS) compared with the control group (Fig. 6 *B* and *C* and Fig. S7*C*). In addition, they displayed higher stiffness compared with horizontally implanted vessels, suggesting that adjustment of the vessel structures to match the orientation of the host tissue vessels improves the functionality and the properties of the resulting tissue.

Discussion

Development of functional and mature blood vessel networks in implantable engineered tissues is fundamental to effective application of tissue engineering techniques toward treatment of a diversity of diseases, such as ischemia and cancer (29, 30). Therefore, much contemporary research focuses on exploring the molecular determinants of the vasculogenesis and angiogenesis processes (31–33). The present study considered the contribution of tensile forces to regulation of formation and overall structure of vascular networks. Three-dimensional polymeric systems seeded with EC and fibroblast cocultures provided the basic conditions necessary for creation of a vessel network. A correlation between the degree of cell-induced contractile forces and the quality of the resulting vessel network was observed. In addition, cyclic and static tensile forces induced distinct effects on network orientation and angiogenic factor secretion. Moreover, organized vascular networks implanted in the mouse abdominal muscle integrated more effectively within the host tissue, compared with nonaligned control samples. Here, we present evidence that the actomyosin pathway, responsible for force generation, with a direct impact on cell shape and tissue remodeling (18, 34–36), guides vascular network assembly. This guidance is achieved via the actin fibers and myosin II, which orient the cells and trigger stretch-induced elongation, respectively (37). Myosin II inhibition resulted in a reversible decrease both in cell forces and in the quality of the resulting network. Moreover, vascular networks formed in fixated gels under ROCK inhibition were impaired, an effect that was not observed in free-floating gels. The dual contribution of ROCK activity to angiogenesis is manifested by tail retraction, leading to enhanced cell migration and further stimulation of angiogenesis, alongside cell cortical tension, resulting in decreased branching and inhibition of angiogenesis (38). Although the role of Myosin II is generally related to cell forces, we further tested response to the inhibitor of ROCK, a protein responsible for mediating cell forces and with a specific role in angiogenesis. In this paper, we present the dual contribution of this inhibitor to the angiogenesis process with and without application of force. Our observations suggest that ROCK activity on a background of cell forces predominantly involves tail retraction and that its inhibition results in decreased migration and damaged vascular networks. In contrast, inhibition of ROCK within the free-floating scaffold results in lower cortical tension, higher branching, and a

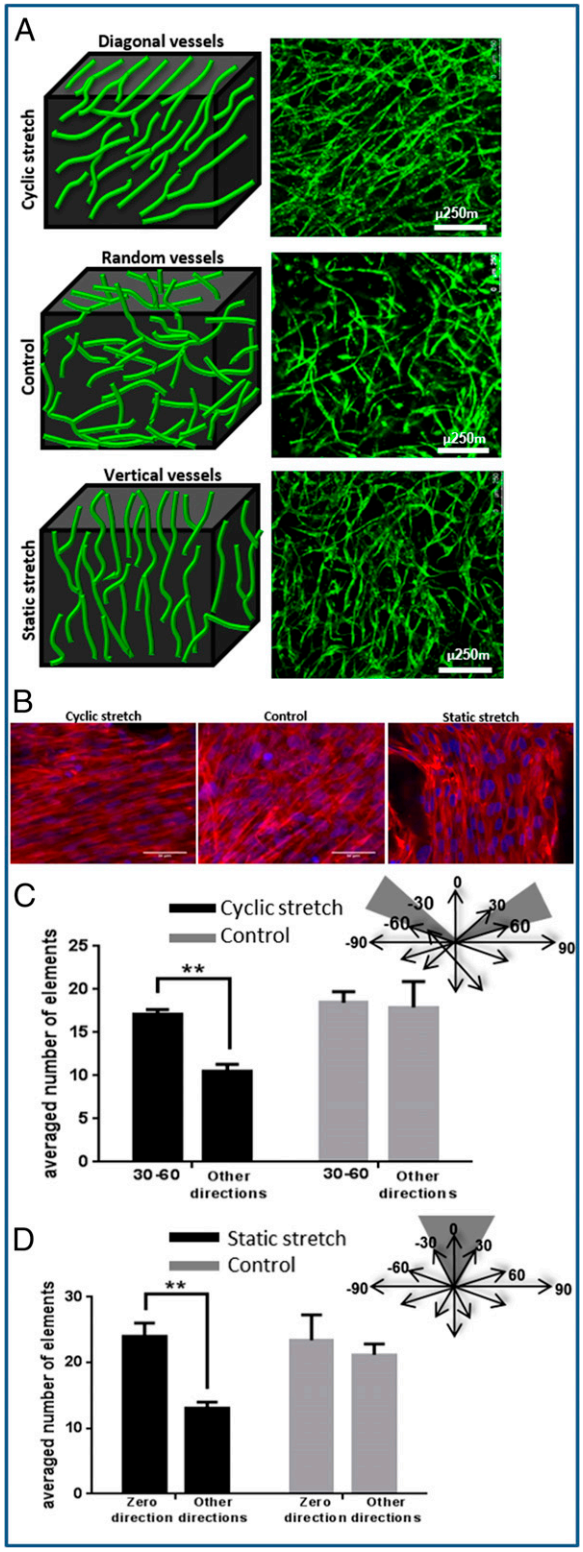

Fig. 3. The orientation of vessel-like structures upon exposure to various mechanical stretching regimens. (*A*) Cyclic stretching applied on uniaxially fixated seeded constructs resulted in diagonal vessels whereas static stretching resulted in vertical vessels, and free-floating scaffolds resulted in randomly orientated vessels. Green, HUVEC-GFP cells. (Scale bars: 250 μm.) The presented images are the projection of about a 500-μm volume. (*B*) The orientation of cell actin fibers upon exposure to the mechanical forces described in *A*. Red, phalloidin staining; blue, DAPI. (*C*) Orientation analysis. Quantification of the average number of objects in 30–60° direction under cyclic stretching and control. (*D*) Orientation analysis. Quantification of the average number of objects in the stretching direction under static stretching and control.

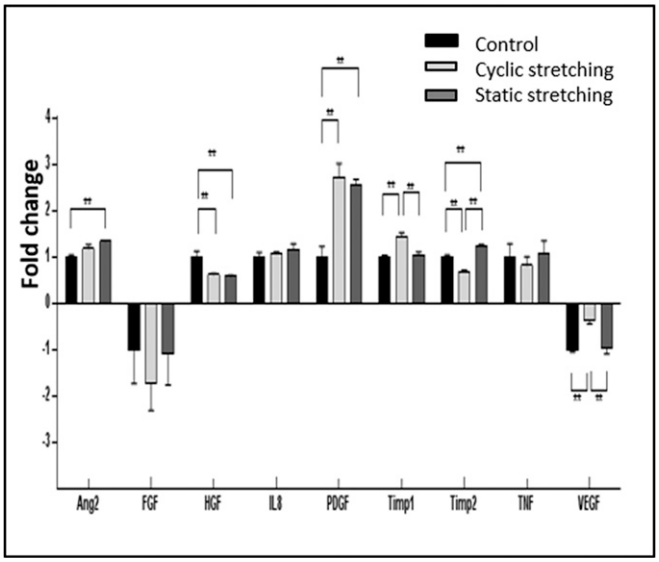

Fig. 4. Secretion of angiogenic proteins by cells under the various mechanical stretching regimens. Angiogenesis-related protein secretion from cell-embedded Gelfoam scaffolds grown under cyclic stretching or static stretching conditions. Medium was collected from all samples on day 8 postseeding. Fold change from the control (no stretch) group (=1) is presented. ***P* value < 0.01.

normal network organization. VEGF is responsible for initiating vessel formation and inducing molecular and cellular events leading to network stabilization and maturation (39). VEGF inhibition in a coculture of ECs and fibroblasts was predicted to damage the network only whereas the level of forces could be maintained by the fibroblasts (19, 40, 41). However, the presented results suggest that the force measured during network assembly is applied by both cell types, which provide a synergistic effect on overall force when collaborating to form elongated tubes. Multicellular organization can be the result of a single cell type driving the orientation of the other cell types or, alternatively, active involvement of both cell types in the orientation process. The current observations imply that both cell types are actively involved in the process because EC damage resulted in decreased forces but had no impact on fibroblast orientation. Furthermore, correlation between the degree of generated force and network quality was also demonstrated upon inhibition of γ-secretase, which did not affect total measured force intensity but shortened the time to achieve maximum force, due to increased angiogenic sprouting induced by the heightened tip cell counts (26). In this study, we demonstrated a means of directing tube assembly using tensile forces, as well as the importance of cell orientation in network structuring. Although other studies have focused on guiding cell orientation using specific patterns or by growing ECs without stromal cell support (11, 42, 43), here, we relied on self-assembly of a coculture of fibroblasts and ECs and observed formation of a stable and mature vascular network, affected only by the applied tensile forces (24, 44). Both static and cyclic forces were examined because they were shown to have differential effects on ECs grown in 2D settings (45). In the present 3D setup, the static forces orientated the cells in the stretching direction whereas the cyclic forces symmetrically oriented the cells 30–60° to the stretching direction, consistent with earlier reports of single-cell observations (46, 47). Importantly, the present model characterized the whole-structure response, and not the single-cell response, to stretching modalities. The contribution of mechanical forces on vascular network morphology and properties can aid in tailoring these responses to match the structure of a desired site of implantation.

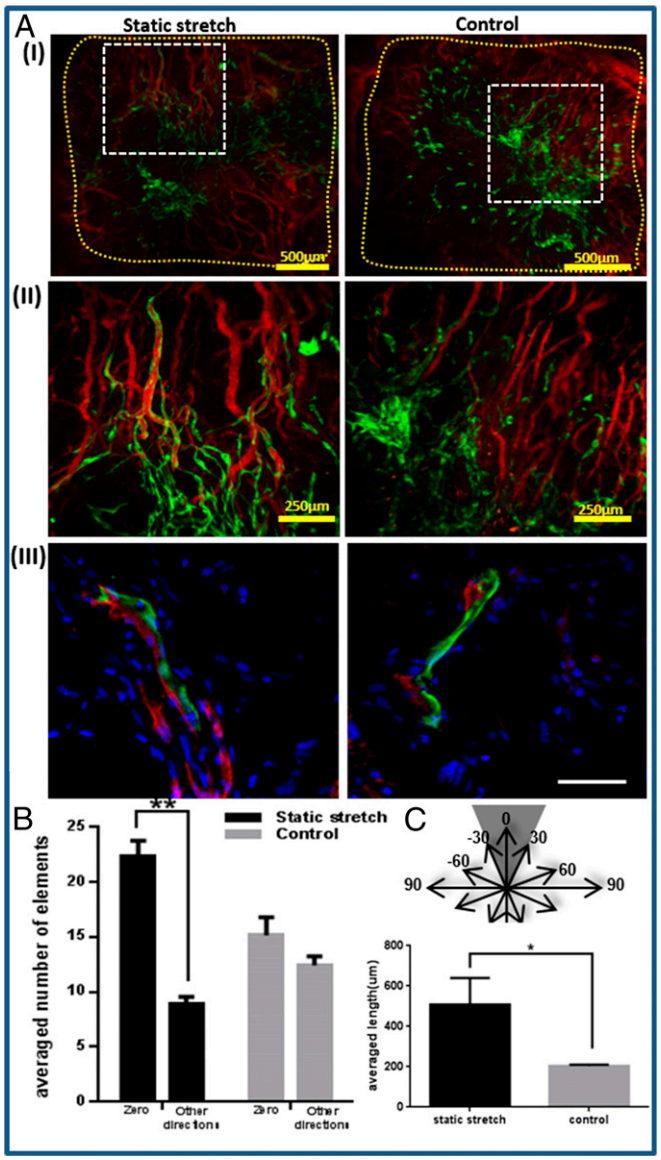

Fig. 5. Implantation of static-stretched and control scaffolds in the mouse abdominal muscle. Scaffolds were implanted on day 8 postseeding. Two weeks thereafter, rhodamine-dextran was injected through the mouse tail vein to view functional vessels. (*A*, *I*) Fluorescence imaging of HUVEC-GFP cells and of rhodamine-dextran in the retrieved scaffolds. Scaffold area is marked in yellow. (*II*) A larger magnification of the retrieved scaffolds, showing a connection between the implanted and the host vascular network, as well as functional implanted vessel-like structures. (*III*) Histological staining of frozen sections of the retrieved scaffold. Green, HUVEC-GFP; red, mouse vessels stained with anti-CD31 antibody; blue, DAPI for nucleic staining. (Scale bar: *III*, 50 μm.) (*B*) Orientation analysis of vessel-like structures 2 wk postimplantation. Objects from static-stretched scaffolds preserved their orientation in the zero direction, compared with the control scaffold, where no dominant direction was observed. (*C*) The mean length of functional implanted vessel-like structures.

Moreover, cyclic stretching was shown to induce a proangiogenic environment, compared with static stretching and the free-floating control. The timing and kinetics of angiogenic factor release (namely, rapid release of VEGF followed by slow release of PDGF-ββ) have been shown to determine network maturity and stabilization (48). In the present experimental setup, VEGF levels were reduced in all configurations, with the highest levels recorded upon cyclic stretching, whereas PDGF-ββ levels increased, with the highest levels measured under cyclic stretching conditions (Fig. 2*E*). These findings correspond with a report of induced autocrine and paracrine signaling in endothelial and stromal cells subjected to cyclic stretching, followed by up-regulation of Ang-2 and PDGF-ββ protein expression (21).

The understanding that mechanical forces influence the internal structure and overall properties of vascular networks can aid in tailoring them to match the structure of a desired site of implantation. Oriented vessel-like structures implanted in the direction of muscle fibers in the line-alba of abdominal muscle preserved their orientation and contained longer functional vessels compared with the nonstretched control, addressing the need to match the implanted engineered tissue structure with the host tissue structure. No pre- versus postimplantation difference in vessel density was observed (Fig. S7*D*). In parallel, a previous study performed in our laboratory has shown that prolonged prevascularization of engineered muscle tissue (21 d in vitro) results in improved orientation and integration in vivo (3). Here, application of tensile forces shortened the required prevascularization period to 7 d in vitro. The 2-wk in vivo incubation period was selected because it was previously shown to be sufficient to observe good integration with the host tissue (3). Shorter incubation intervals of 3–4 d in vivo would not be sufficient for examination of the functionality of the implanted vessels. Periods longer than 2 wk may not be able to determine whether such orientation matching can accelerate integration of the implanted tissue with the host tissue. Moreover, these results shed light on the involvement of tensile forces in vascularization and on the mechanism underlying force buildup during network assembly. This work presents a means of achieving vascularized engineered tissues with properties and structures supportive of host tissue function and viability and can be broadened to obtain different arrangements of vascular networks to match those of diverse tissues, such as cardiac, retina, and kidney. We demonstrated both the ability to control tube orientation via manipulation of tensile forces and the efficacy of oriented vascularized tissues in tissue transplantation. Most importantly, this approach monitored tissue structure responses, rather than single-cell

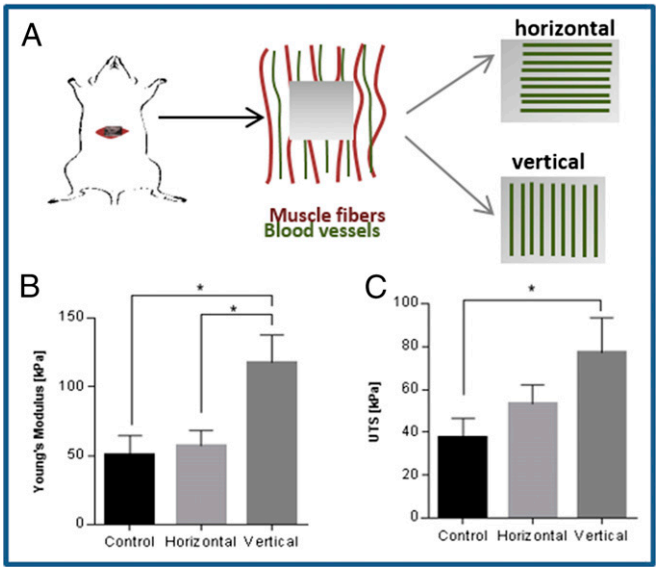

Fig. 6. Mechanical analysis of the implantation site postimplantation. (*A*) Oriented vessels were implanted parallel vs. perpendicular to the vessels of the abdominal tissue. (*B*) The stiffness (Young's modulus) and (*C*) UTS of the tissue 14 d postimplantation, comparing vertical ($n = 6$), horizontal ($n = 4$) and control group ($n = 4$) vessels. *P value < 0.05, **P value < 0.01.

responses, enhancing the understanding of coordinated multicellular responses to environmental signals.

Materials and Methods

Detailed materials and methods are in *SI Materials and Methods*. Briefly, 3D vascular networks were generated by coseeding endothelial cells and fibroblasts on gelatin-based sponges (Gelfoam compressed; Pharmacia & Upjohn Company). Mechanical stimulations were applied on the constructs.

Cyclic Stretching. Cell-embedded Gelfoam scaffolds were cultured for 4 d and then transferred for another 4 d to the Biodynamic test instrument (Electroforce; Bose), where uniaxial cyclic stretching of 10% strain and 1-Hz frequency was applied. Strain was calculated as change in length divided by initial length of the sample.

Static Stretching. Constructs were fixated within a self-designed fixation device, followed by cell seeding.

Control Group. Cell-embedded constructs were grown in a plate.

Cocultures of endothelial cells and fibroblasts were also used to create 3D vascular networks within uniaxial fixated or nonfixated fibrin gels. The cell-embedded fibrin gels were created between two PDMS μposts (Myomics). Control groups included cell-embedded fibrin gels grown within 48-well plates, either attached to the plate or in a free-floating state. Whole human umbilical vein endothelial cell (HUVEC)-green fluorescent protein GFP–seeded Gelfoam constructs and fibrin gels were imaged. Both network quality and vessel-like structure orientation were estimated. Eight days postseeding, static stretched and control scaffolds were implanted in the abdominal muscle of mice. All animal studies were approved by the Committee on the Ethics of Animal Experiments of the Technion.

ACKNOWLEDGMENTS. We thank Inbal Michael for help with the cytokine analysis and Yehudit Posen for proofreading the article. The research leading to these results has received funding from the European Research Council (ERC) under the European Union's Seventh Framework Program (FP/2007-2013), ERC Grant Agreement 281501-ENGVASC and Grant Agreement 229294-NanoCard, and was supported in part by the Russell Berrie Nanotechnology Institute at the Technion-Israel Institute of Technology.

1. Novosel EC, Kleinhans C, Kluger PJ (2011) Vascularization is the key challenge in tissue engineering. *Adv Drug Deliv Rev* 63(4-5):300–311.
2. Shandalov Y, et al. (2014) An engineered muscle flap for reconstruction of large soft tissue defects. *Proc Natl Acad Sci USA* 111(16):6010–6015.
3. Koffler J, et al. (2011) Improved vascular organization enhances functional integration of engineered skeletal muscle grafts. *Proc Natl Acad Sci USA* 108(36):14789–14794.
4. Takebe T, et al. (2013) Vascularized and functional human liver from an iPSC-derived organ bud transplant. *Nature* 499(7459):481–484.
5. Caspi O, et al. (2007) Tissue engineering of vascularized cardiac muscle from human embryonic stem cells. *Circ Res* 100(2):263–272.
6. Kaufman-Francis K, Koffler J, Weinberg N, Dor Y, Levenberg S (2012) Engineered vascular beds provide key signals to pancreatic hormone-producing cells. *PLoS One* 7(7):e40741.
7. Santos MI, Reis RL (2010) Vascularization in bone tissue engineering: Physiology, current strategies, major hurdles and future challenges. *Macromol Biosci* 10(1):12–27.
8. Chung JC, Shum-Tim D (2012) Neovascularization in tissue engineering. *Cells* 1(4): 1246–1260.
9. Lesman A, et al. (2011) Engineering vessel-like networks within multicellular fibrin-based constructs. *Biomaterials* 32(31):7856–7869.
10. Miller JS, et al. (2012) Rapid casting of patterned vascular networks for perfusable engineered three-dimensional tissues. *Nat Mater* 11(9):768–774.
11. Baranski JD, et al. (2013) Geometric control of vascular networks to enhance engineered tissue integration and function. *Proc Natl Acad Sci USA* 110(19):7586–7591.
12. Dado-Rosenfeld D, Tzchori I, Fine A, Chen-Konak L, Levenberg S (2015) Tensile forces applied on a cell-embedded three-dimensional scaffold can direct early differentiation of embryonic stem cells toward the mesoderm germ layer. *Tissue Eng Part A* 21(1-2): 124–133.
13. Fletcher DA, Mullins RD (2010) Cell mechanics and the cytoskeleton. *Nature* 463(7280):485–492.
14. Abu Shah E, Keren K (2013) Mechanical forces and feedbacks in cell motility. *Curr Opin Cell Biol* 25(5):550–557.
15. Krieg M, et al. (2008) Tensile forces govern germ-layer organization in zebrafish. *Nat Cell Biol* 10(4):429–436.
16. Hoffman BD, Grashoff C, Schwartz MA (2011) Dynamic molecular processes mediate cellular mechanotransduction. *Nature* 475(7356):316–323.
17. Balaban NQ, et al. (2001) Force and focal adhesion assembly: A close relationship studied using elastic micropatterned substrates. *Nat Cell Biol* 3(5):466–472.
18. DuFort CC, Paszek MJ, Weaver VM (2011) Balancing forces: Architectural control of mechanotransduction. *Nat Rev Mol Cell Biol* 12(5):308–319.
19. Dado D, Levenberg S (2009) Cell-scaffold mechanical interplay within engineered tissue. *Semin Cell Dev Biol* 20(6):656–664.
20. Milde F, Lauw S, Koumoutsakos P, Iruela-Arispe ML (2013) The mouse retina in 3D: Quantification of vascular growth and remodeling. *Integr Biol (Camb)* 5(12):1426–1438.
21. Yung YC, Chae J, Buehler MJ, Hunter CP, Mooney DJ (2009) Cyclic tensile strain triggers a sequence of autocrine and paracrine signaling to regulate angiogenic sprouting in human vascular cells. *Proc Natl Acad Sci USA* 106(36):15279–15284.
22. Dickinson LE, Rand DR, Tsao J, Eberle W, Gerecht S (2012) Endothelial cell responses to micropillar substrates of varying dimensions and stiffness. *J Biomed Mater Res A* 100(6): 1457–1466.
23. Vandenburgh H, et al. (2008) Drug-screening platform based on the contractility of tissue-engineered muscle. *Muscle Nerve* 37(4):438–447.
24. Kaully T, Kaufman-Francis K, Lesman A, Levenberg S (2009) Vascularization: The conduit to viable engineered tissues. *Tissue Eng Part B Rev* 15(2):159–169.
25. Keskin U, Totan Y, Karadağ R, Erdurmuş M, Aydın B (2012) Inhibitory effects of SU5416, a selective vascular endothelial growth factor receptor tyrosine kinase inhibitor, on experimental corneal neovascularization. *Ophthalmic Res* 47(1):13–18.
26. Hellström M, et al. (2007) Dll4 signalling through Notch1 regulates formation of tip cells during angiogenesis. *Nature* 445(7129):776–780.
27. Ando J, Yamamoto K (2011) Effects of shear stress and stretch on endothelial function. *Antioxid Redox Signal* 15(5):1389–1403.
28. Ngu H, et al. (2010) Effect of focal adhesion proteins on endothelial cell adhesion, motility and orientation response to cyclic strain. *Ann Biomed Eng* 38(1): 208–222.
29. Losordo DW, Dimmeler S (2004) Therapeutic angiogenesis and vasculogenesis for ischemic disease. Part II. Cell-based therapies. *Circulation* 109(22):2692–2697.
30. Welti J, Loges S, Dimmeler S, Carmeliet P (2013) Recent molecular discoveries in angiogenesis and antiangiogenic therapies in cancer. *J Clin Invest* 123(8):3190–3200.
31. Potente M, Gerhardt H, Carmeliet P (2011) Basic and therapeutic aspects of angiogenesis. *Cell* 146(6):873–887.
32. Carmeliet P (2000) Mechanisms of angiogenesis and arteriogenesis. *Nat Med* 6(4): 389–395.
33. Buschmann I, Schaper W (1999) Arteriogenesis versus angiogenesis: Two mechanisms of vessel growth. *News Physiol Sci* 14:121–125.
34. Kasza KE, Zallen JA (2011) Dynamics and regulation of contractile actin-myosin networks in morphogenesis. *Curr Opin Cell Biol* 23(1):30–38.
35. Salbreux G, Charras G, Paluch E (2012) Actin cortex mechanics and cellular morphogenesis. *Trends Cell Biol* 22(10):536–545.
36. Munjal A, Lecuit T (2014) Actomyosin networks and tissue morphogenesis. *Development* 141(9):1789–1793.
37. Greiner AM, Chen H, Spatz JP, Kemkemer R (2013) Cyclic tensile strain controls cell shape and directs actin stress fiber formation and focal adhesion alignment in spreading cells. *PLoS One* 8(10):e77328.
38. van Nieuw Amerongen GP, van Hinsbergh VW (2009) Role of ROCK I/II in vascular branching. *Am J Physiol Heart Circ Physiol* 296(4):H903–H905.
39. Carmeliet P, Jain RK (2011) Molecular mechanisms and clinical applications of angiogenesis. *Nature* 473(7347):298–307.
40. Lesman A, Notbohm J, Tirrell DA, Ravichandran G (2014) Contractile forces regulate cell division in three-dimensional environments. *J Cell Biol* 205(2):155–162.
41. Li B, Wang JHC (2011) Fibroblasts and myofibroblasts in wound healing: Force generation and measurement. *J Tissue Viability* 20(4):108–120.
42. Lai ES, Huang NF, Cooke JP, Fuller GG (2012) Aligned nanofibrillar collagen regulates endothelial organization and migration. *Regen Med* 7(5):649–661.
43. van der Schaft DW, van Spreeuwel AC, van Assen HC, Baaijens FP (2011) Mechanoregulation of vascularization in aligned tissue-engineered muscle: A role for vascular endothelial growth factor. *Tissue Eng Part A* 17(21-22):2857–2865.
44. Rouwkema J, Rivron NC, van Blitterswijk CA (2008) Vascularization in tissue engineering. *Trends Biotechnol* 26(8):434–441.
45. Zheng W, Christensen LP, Tomanek RJ (2008) Differential effects of cyclic and static stretch on coronary microvascular endothelial cell receptors and vasculogenic/angiogenic responses. *Am J Physiol Heart Circ Physiol* 295(2):H794–H800.
46. Livne A, Bouchbinder E, Geiger B (2014) Cell reorientation under cyclic stretching. *Nat Commun* 5:3938.
47. De R, Zemel A, Safran SA (2007) Dynamics of cell orientation. *Nat Phys* 3(9):655–659.
48. Richardson TP, Peters MC, Ennett AB, Mooney DJ (2001) Polymeric system for dual growth factor delivery. *Nat Biotechnol* 19(11):1029–1034.